Climate Dynamics (2025) 63:340
https://doi.org/10.1007/s00382-025-07829-y

ORIGINAL ARTICLE

Characteristics of widespread extreme precipitation events in Peninsular Spain and the Balearic Islands: spatio-temporal dynamics and driving mechanisms

Sergio M. Vicente-Serrano[1,2] · Jose M. Garrido-Perez[3] · José Carlos Fernández-Álvarez[4,5] · Luis Gimeno-Sotelo[6,7] · Santiago Beguería[2,8] · Amar Halifa-Marín[1,2] · Borja Latorre[2,8] · Ahmed M. El Kenawy[1,2] · Magí Franquesa[1,2] · María Adell-Michavila[1,2] · Fernando Domínguez-Castro[1,2] · David Barriopedro[9] · Luis Gimeno-Presa[4,5,10] · Raquel Nieto[4,5,10] · Cesar Azorin-Molina[11] · Miguel Andres-Martin[11] · Jose Manuel Gutiérrez[12] · Ricardo García-Herrera[3]

Received: 4 March 2025 / Accepted: 24 July 2025

Abstract

This study analysed widespread extreme precipitation events (WEPEs) across Spain using a high-density network of daily precipitation records, aiming to clarify their spatiotemporal trends and drivers. The findings reveal that WEPEs in Spain show a non-significant trend in either frequency or intensity since 1961, despite the prevailing trend of global warming. Nevertheless, atmospheric circulation plays a key role in shaping WEPEs in Spain, with five distinct synoptic patterns driving extreme precipitation across different regions. Westerly flows associated with Atlantic lows lead to widespread precipitation in northern and western Spain, while cut-off lows generate intense but more localized events, particularly in the east. Jet stream anomalies and moisture transport patterns, particularly from the Mediterranean and Atlantic, further modulate the spatial distribution and intensity of WEPEs, highlighting the interaction between regional and large-scale climatic drivers. These findings highlight the importance of distinguishing between widespread and localized EPEs and the associated atmospheric mechanisms.

✉ Sergio M. Vicente-Serrano
svicen@ipe.csic.es

[1] Instituto Pirenaico de Ecología, Consejo Superior de Investigaciones Científicas (IPE- CSIC), Zaragoza, Spain

[2] Laboratorio de Climatología y Servicios Climáticos (LCSC), CSIC-University of Zaragoza, Zaragoza, Spain

[3] Departamento de Física de la Tierra y Astrofísica, Facultad de Ciencias Físicas, Universidad Complutense de Madrid, Madrid, Spain

[4] Galicia Supercomputing Center (CESGA), Santiago de Compostela, Spain

[5] Centro de Investigación Mariña, Environmental Physics Laboratory (EPhysLab), Universidade de Vigo, Ourense, Spain

[6] Departamento de Estatística e Investigação Operacional, Faculdade de Ciências, Universidade de Lisboa, Lisboa, Portugal

[7] CEAUL - Centro de Estatística e Aplicações, Faculdade de Ciências, Universidade de Lisboa, Lisboa, Portugal

[8] Estación Experimental de Aula Dei, Consejo Superior de Investigaciones Científicas EEAD-CSIC, Zaragoza, Spain

[9] Instituto de Geociencias (CSIC-UCM), Madrid, Spain

[10] Unidad Asociada, CSIC-Universidad de Vigo: Grupo de Física de la Atmósfera y del Océano, Pontevedra, Spain

[11] Centro de Investigaciones sobre Desertificación, Climate, Atmosphere and Ocean Laboratory (Climatoc-Lab), Consejo Superior de Investigaciones Científicas (CIDE, CSIC-UV-Generalitat Valenciana), Moncada, Valencia, Spain

[12] Instituto de Física de Cantabria, Consejo Superior de Investigaciones Científicas (IFCA-CSIC), Santander, Spain

Published online: 30 August 2025

1 Introduction

The Mediterranean region, particularly southwestern Europe, is increasingly recognized as a climate hotspot due to its vulnerability to global climate change (Cramer et al. 2018; Lionello and Scarascia 2020; Doblas-Reyes et al. 2021). Southwestern Europe, encompassing Spain, Portugal, and parts of southern France, frequently experiences extreme precipitation events (EPEs) (Ribes et al. 2019; Miró et al. 2022), with adverse impacts on the environment, infrastructure, and human life (White et al. 1997; Llasat et al. 2013). EPEs often consist of short, intense rainfall episodes that trigger catastrophic flooding, landslides, and damage to infrastructure. These impacts are especially pronounced in mountainous areas and along the Mediterranean coastlines, where orography plays a key role in triggering convective processes that amplify rainfall intensity, particularly at the end of the summer season when upper-atmosphere cold air masses encounter warm Mediterranean sea surface temperatures (Llasat et al. 2013; Ramis et al. 2013). In other cases, EPEs encompasses prolonged periods of anomalous intense rainfall over consecutive days, resulting in gradual flooding in certain basins (Peña et al. 2022).

EPEs pose significant long-term challenges for water resource management, agriculture, and urban planning in Spain (Olcina Cantos and Díez-Herrero 2017). As population growth and urban expansion continues, an increasing number of people and assets are exposed to the risks associated with EPEs, intensifying community vulnerability (Cortès et al. 2018; Roldán-Valcarce et al. 2023; Cánovas-García and Vargas Molina 2024). Assessing these events is therefore critical in climate research, not only for understanding their mechanisms but also for developing effective mitigation and adaptation strategies (Gimeno et al. 2022).

There is ongoing debate about trends in EPEs worldwide. Some studies suggest that heavy precipitation events are increasing globally due to thermodynamic factors associated with recent global warming (Lehmann et al. 2015; Papalexiou and Montanari 2019; Seneviratne et al. 2021). This increase is estimated to follow the Clausius-Clapeyron relationship, with a rate of approximately 6–7% per one degree of warming (Chen et al. 2019; Fowler et al. 2021). However, this mechanism remains uncertain in observations, as it relies on the assumption of constant relative humidity. Recent studies have highlighted potential challenges to this assumption (Byrne and O'Gorman 2018), including observed declines in relative humidity in some regions, such as southwestern Europe (Vicente-Serrano et al. 2014).

Moreover, other factors, particularly atmospheric dynamics, are crucial in determining the occurrence and timing of EPEs across different spatial scales (Gimeno et al. 2022). These may include shifts in low-level jets, the storm track or the frequency of atmospheric rivers, which may impact EPE patterns in ways that cannot be solely attributed to thermodynamic effects (Eiras-Barca et al. 2018; Gimeno-Sotelo and Gimeno 2023). As a result, while thermodynamic mechanisms suggest a global trend toward more frequent and intense precipitation, the role of changes in atmospheric dynamics introduces additional complexities, particularly in regions like southwestern Europe where both mechanisms interact uniquely. This complex interplay between thermodynamic and dynamic factors highlights the need for regional-scale analysis to achieve a better understanding of EPE dynamics.

In southwestern Europe, some studies have suggested an increase in EPEs. For example, Ribes et al. (2019) reported a rise in extreme precipitation events in this region, although the signal varies across subregions. In Spain, research has suggested increasing storm activity over the past 50 years, especially during autumn and winter, which would increase the frequency of severe precipitation events (Camarasa-Belmonte et al. 2020; Miró et al. 2022). However, most studies across the Iberian Peninsula have reported non-significant long-term trends in extreme precipitation, suggesting a generally stationary pattern. These results were found using multidecadal station (Beguería et al. 2011; Hidalgo-Muñoz et al. 2011; Gallego et al. 2011; Merino et al. 2016) and gridded data (Serrano-Notivoli et al. 2018). However, analyses based on point observations or gridded data struggle to capture the dynamics of these extreme events due to their low frequency and spatial randomness (García-Ruiz et al. 2000). In Spain, this challenge is further compounded by the climatological characteristics of the region: severe precipitation events are not only infrequent but also exhibit high spatial variability when they do occur. While in the Mediterranean region most of the EPEs have their origin in local and mesoscale phenomena, in the rest of the country, EPEs are usually associated with synoptic scale processes. These factors, combined with the inherent difficulties of analyzing daily rainfall records, make it particularly challenging to determine whether the intensity or frequency of extreme precipitation has changed in recent decades. This highlights the need for regional-scale assessments to better understand the probability of EPEs and potential trends in their severity (Ribes et al. 2019).

The complexity of EPEs dynamics is shaped by the country's unique geographical features, where topography interacts with atmospheric mechanisms (Romero et al. 1997; Peñarrocha et al. 2002) and thermodynamic drivers, including Mediterranean sea surface temperatures (Pastor et al. 2001). Research on EPEs in Spain has largely focused on the eastern Mediterranean regions (Homar et al. 2002; Ferreira 2021; Hermoso et al. 2021), which typically record the

most intense rainfall; however, long-term trends in the frequency and severity of these events remain underexplored. While several comprehensive studies have investigated the mechanisms behind EPEs in Spain, most of them are limited to specific events or regions near the Mediterranean Sea, where the most extreme events occur (Romero et al. 1999a, b; Ramis et al. 2013; Pérez-Zanón et al. 2018; Miró et al. 2022). To overcome these limitations, we provide a comprehensive assessment of the spatial and temporal variability of widespread EPEs (WEPEs) across the whole of Spain and their driving mechanisms. Our assessment employs the most complete and multidecadal record of daily precipitation available for Spain. Importantly, our study presents a novel methodology that aims to overcome existing limitations in trend assessment.

2 Data and methods

2.1 Data

We used data from 2292 daily precipitation stations from 1961 to 2022 (Fig. 1a), selected from the complete set of daily precipitation records available from the Spanish Meteorological Agency (AEMET), which includes raw data from almost 11,000 stations. This dataset underwent rigorous quality control (Vicente-Serrano et al. 2010), and series containing more than 35 years of original data were reconstructed using a quantile matching approach based on neighbouring stations (Beguería et al. 2019). For this reconstruction, only series with at least a 15-year overlap and located within a 50 km radius of the target station were considered. On average, 21.7% of the data in each precipitation series was filled. However, the majority of the stations had a much lower proportion of filled data, with most series requiring less than 5% infilling (Fig. 1b).

To analyze the atmospheric patterns associated with WEPEs, we employed daily geopotential height at 500 hPa (Z500), zonal and meridional wind at 850 hPa, and zonal wind at 925–700 hPa. The Z500 data were used to create climatological composites and categorize the atmospheric circulation patterns through weather regimes (WRs), the wind at 850 hPa was used for composites, and the zonal wind at 925–700 hPa was used to characterize the North Atlantic eddy-driven jet (EDJ). To characterize the synoptic context of extreme precipitation events, we used 500 hPa geopotential height fields, as they provide a robust representation of large-scale atmospheric circulation patterns. Unlike sea-level pressure (SLP), which often reflects more local and topographically influenced features, 500 hPa geopotential height fields captures mid-tropospheric dynamics that govern the development and movement of weather systems over broader regions. This makes it particularly suitable for identifying the main drivers of extreme precipitation affecting large spatial domains, which is the focus of this study.

Further details on the definition of WRs and EDJ can be found in Sect. 2.3. For this purpose, we employed the ERA5 reanalysis, provided by the European Centre for Medium-Range Weather Forecasts (ECMWF), for 1961–2022 (Hersbach et al. 2020). The same dataset for 1981–2022 was used to obtain daily data for the following variables at a 0.5° resolution: precipitation, vertically-integrated horizontal moisture transport (IVT), vertically-integrated water vapor (IWV), and vertical velocity at 500 hPa. The analysis of these variables was limited to this shorter period to reduce inconsistencies in humidity conditions associated with the pre-satellite era.

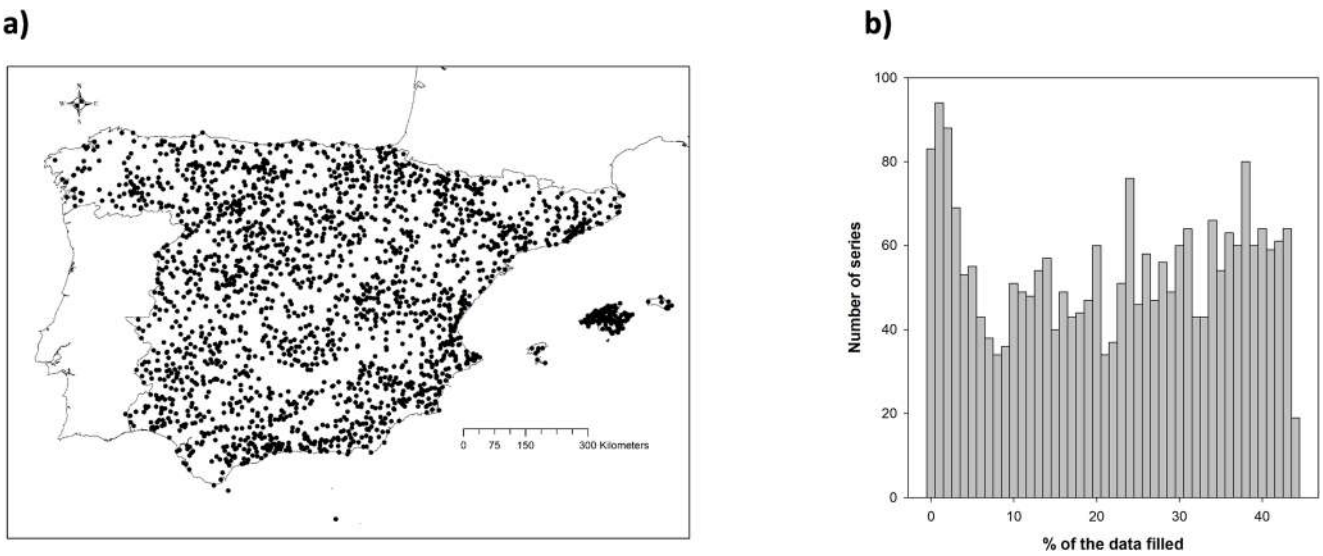

Fig. 1 **a** Spatial distribution of the precipitation stations used in this study and **b** number of precipitation series by percentage of data filled

Furthermore, to analyze the moisture sources for WEPEs, we employed the data from the simulations of FLEXible PARTicle dispersion model (FLEXPARTv10.4, Stohl et al. 2005; Pisso et al. 2019) also forced with ERA5 with a horizontal resolution of 0.5° × 0.5° and 137 vertical levels at synoptic times from 1980 to 2022. In the FLEXPART simulations, the atmosphere was divided into approximately 30 million parcels and released and dispersed globally homogeneously following the 3D wind fields, hence the mass of each parcel is the same (Vázquez et al. 2024). The FLEXPART model has been widely applied to identify moisture sources in several earlier studies (Gimeno et al. 2020; Vázquez et al. 2024).

2.2 Definition of WEPEs

To identify days characterized by extreme precipitation affecting large areas of Spain, we first transformed the daily precipitation records into their corresponding empirical percentiles, excluding zero precipitation values. Different criteria can be applied to identify EPEs (Donat et al. 2013a; Alexander et al. 2020). In this study, we set a threshold based on the 99th percentile of each station's precipitation series, recording events based on the proportion of stations exceeding this threshold on a given day. The selection of an appropriate threshold to define EPEs is a critical issue. While a larger sample would indeed help reduce uncertainties in assessing the atmospheric mechanisms underlying specific spatial configurations of extreme precipitation events, using low thresholds (e.g., the 95th percentile) introduces other problems. This threshold corresponds to relatively low precipitation values at some of the meteorological stations considered (Fig. S1a), resulting in the inclusion of events with limited magnitude. Moreover, applying the 95th percentile leads to an unrealistically high number of "extreme" events at several stations (Fig. S1b), which contradicts the fundamental definition of extremes as rare occurrences.

Using the 99th percentile threshold resolves many of these issues: it selects events with generally higher magnitudes and significantly reduces the frequency of identified extremes. While there is room for debate over whether the 99th percentile fully captures true extreme precipitation events, there is little doubt that lower percentiles (e.g., the 95th) represent too low a threshold in the vast majority of cases.

We tested four possible criteria: days when 2.5%, 5%, 10%, or 20% of all stations recorded precipitation above the 99th percentile. Table 1 shows the number of events identified under each tested threshold. We found that the 2.5% threshold was insufficient to identify widespread events over our domain, while the 10% and 20% criteria yielded too few events. Therefore, we selected days on which at least 5%

Table 1 Number of days based on different thresholds, determined by the percentage of stations (relative to the total) recording daily precipitation exceeding the 99th percentile

	Jan.	Feb.	Mar.	Apr.	May	Jun.	Jul.	Aug.	Sep.	Oct.	Nov.	Dec.	Total
2.5% stations	42	15	27	24	14	13	5	9	62	85	87	61	444
5% stations	9	4	2	5	3	5	0	1	14	18	22	25	108
10% stations	1	0	0	0	0	0	0	0	2	4	3	3	13
15% stations	0	0	0	0	0	0	0	0	1	1	2	3	7

of stations recorded precipitation above the 99th percentile, resulting in a total of 108 days. These events predominantly occurred between September and February, with the highest frequency observed in December.

We analyzed the temporal distribution of stations recording precipitation above the 99th percentile and mapped selected days to illustrate the strong spatial diversity that characterizes these events. This spatial diversity was summarized through Principal Component Analysis (PCA) (Richman 1986; White et al. 1991), using daily precipitation values transformed to percentiles to identify the most common spatial patterns associated with these WEPEs across Spain. In climatological studies, two modes of PCA can be applied (S and T) (Serrano et al. 1999). We applied a T-mode Principal Component Analysis (PCA) because our goal was to identify the dominant spatial patterns associated with extreme precipitation events in Spain, rather than to regionalize the territory based on precipitation dynamics. T-mode PCA is specifically suited for this purpose, as it treats the days with extreme events as variables and the meteorological stations as cases, allowing us to detect recurrent spatial configurations of precipitation associated with these events. The resulting principal components represent distinct spatial patterns, and the loadings (Pearson's r correlations) indicate how strongly each event day corresponds to each pattern. In contrast, an S-mode PCA—where stations are treated as variables and daily observations as cases—would have been appropriate if our aim had been to identify regions with similar temporal precipitation behavior. This approach highlights common time series evolution across stations, making it suitable for regionalization but not for detecting spatial patterns linked to specific extreme events. Thus, T-mode PCA provides a robust framework for summarizing and interpreting the spatial organization of extreme precipitation days, which aligns with the core objective of this study.

2.3 Characterization of atmospheric mechanisms

Herein, we analyzed the atmospheric patterns associated with WEPEs using two complementary approaches: (1) the analysis of composites of Z500 and 850 hPa wind anomalies to identify the synoptic patterns directly linked to WEPEs, and (2) a detailed characterization of the North Atlantic eddy-driven jet (EDJ). The identification and characterization of the North Atlantic EDJ are based on the low-pass filtered zonal wind averaged between 925 and 700 hPa over the [120°W–60°E, 15°N–75°N] domain, following the methodology described in Barriopedro et al. (2023). The EDJ, in turn, largely determines the path and intensity of the North Atlantic storm track, which are of particular importance given that periods of a highly wavy jet configuration are often associated with the development of large-scale disruptions in the general circulation, which are particularly relevant for the occurrence of intense precipitation over Iberia, such as cut-off lows (Barriopedro et al. 2023). We used four parameters: intensity, latitudinal position, eastward extension, and tilt. This approach extends the detection of EDJ parameters to additional longitudinal sectors, producing a two-dimensional gridded binary field that marks the latitude of the EDJ core for each longitude and day. In this study, these daily fields are employed to generate anomaly frequency maps of the EDJ, allowing for an analysis of its structure for different components of the WEPEs.

To identify mechanisms at smaller spatial scales that may explain the dynamics of some WEPEs, we calculated anomalies of IVT, atmospheric instability (estimated as vertical velocity ($-\omega$), where positive values indicate upward vertical motion), and TCWV for the WEPEs for 1980–2022. Details for the calculation methods to obtain these variables from ERA5 data can be found in Gimeno-Sotelo et al. (2023).

Finally, to determine the origin and anomaly of the moisture linked to each WEPE, we used the FLEXPART model forced with the ERA5 reanalysis in the period 1980–2022. The anomaly for each WEPE day was calculated as the difference between the moisture sources for that specific day and the climatology of that day across all years under consideration. To estimate the moisture sources, we used the trajectories from the FLEXPART experiment. We applied a Lagrangian methodology (Stohl and James 2004) to follow the changes in the specific moisture content (q) over time (every 6 h) along the tracks described by each atmospheric particle in which the atmosphere was divided into. The particle trajectories were followed for 10 days prior to the day of occurrence of the WEPE, which is the considered average residence time of water vapour particles in the atmosphere (Gimeno et al. 2021). Also, we consider those particles that have experienced a decrease in specific humidity greater than 0.1 g/kg in the 6 h before reaching the target region in which the WEPE occurs, in line with the approach set out by Läderach and Sodemann (2016). Then, the values for each grid are added to calculate the moisture source pattern. The lagrangian trajectories post-processing was carried out using the TRansport Of water Vapour (TROVAv1.0) software (Fernández-Alvarez et al. 2022).

3 Results

3.1 Spatio-temporal variability of the precipitation events

In a typical year, several stations record daily precipitation values above the 99th percentile. However, it is less common for a substantial number of stations to simultaneously exceed this threshold on the same day (Fig. 2). Over the analyzed period, no days were recorded when more than 25% of Spain had precipitation above the 99th percentile, indicating that WEPEs are generally localized and affect limited areas of the country. In rare instances, a large portion of Spain experiences WEPEs. Notable examples include November 5, 1982; November 5, 1997; December 24–27, 2013; and December 19, 2019, during which over 20% of weather stations recorded daily precipitation exceeding the 99th percentile.

Regardless of the threshold chosen to identify days with WEPEs, the annual frequency of such days does not show statistically significant trends (Mann-Kendall test, $p<0.05$) (Figure S1), suggesting that the frequency of days with WEPEs remains stable in mainland Spain. Additionally, using a threshold of 5%, not only is there no increase in the number of days with a high percentage of stations recording EPEs, but the magnitude of precipitation on these days also shows no significant change. The box plots of daily precipitation associated with the WEPEs according to a threshold of 5% remain stable across the different decades (Fig. 3).

The spatial patterns of precipitation on these days exhibit significant variability across regions (Figure S3). Some days show WEPEs across the country (e.g., 19 December 1980, 6 November 1982), but it is more common for extreme precipitation to affect only portions of Spain, such as the North (16 December 1989), Southeast (2 November 2015), or Northwest (23 October 2000). Despite these varied spatial patterns, certain dominant configurations emerge in the occurrence of WEPEs in Spain. The results of the PCA indicate that three components explain most of the total variance (Fig. S4). Specifically, the first three components account for the majority of the total variance (51.1%) and reveal distinct spatial patterns: a west-east gradient in the first component (Fig. 4a), a north-south gradient in the second (Fig. 4b), and a separation between central and northwestern versus southeastern areas in the third (Fig. 4c). The remaining components exhibit more localized patterns.

According to the maximum loading rule, the majority of WEPEs align with the configuration represented by component 1, covering 72 days (60 with positive loading and 12 with negative loading) (Fig. 4d). The evolution of this component shows a nearly constant pattern, with frequent occurrences throughout the period, though days associated with the negative phase (extreme precipitation in the southeast) have become more common in the last two decades. Days exhibiting the spatial configurations of component 2 are also frequent and include both positive and negative phases (Fig. 4e). In contrast, for component 3, only the positive phase represents a substantial number of days (Fig. 4f). The remaining components account for a very small number of days, thus providing limited insight into the variability of WEPEs in Spain. Consequently, the analysis of atmospheric mechanisms controlling generalized extreme precipitation days focuses on five spatial configurations: two for components 1 and 2 (positive and negative phases) and one for the positive phase of component 3.

3.2 Atmospheric circulation and instability, and air humidity transport of extreme precipitation days

Here, we provide an assessment of the atmospheric mechanisms and moisture sources associated with the most typical spatial configurations that accompany WEPEs over Spain.

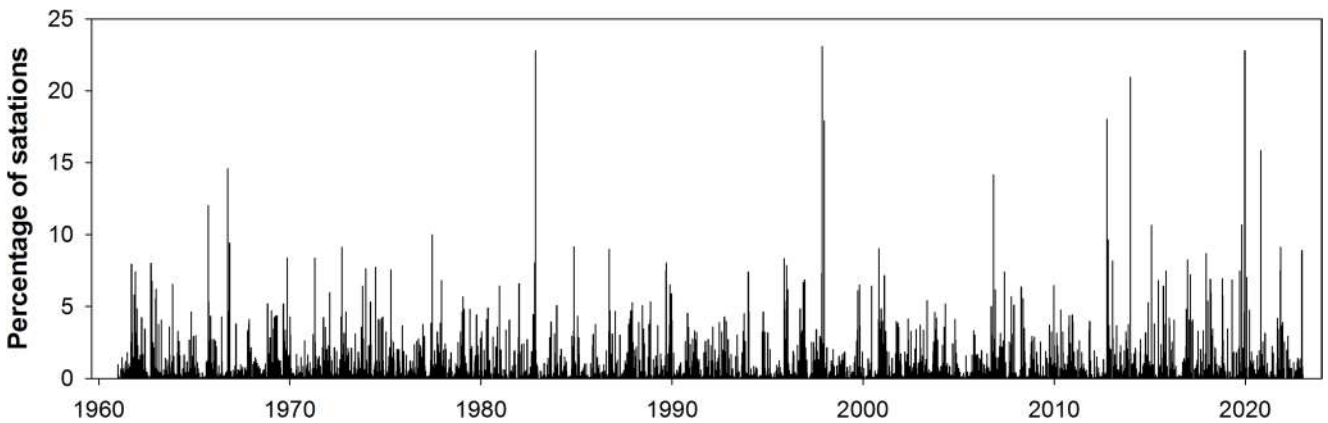

Fig. 2 Evolution of the daily percentage of stations above the 99th percentile over Spain (1961–2022)

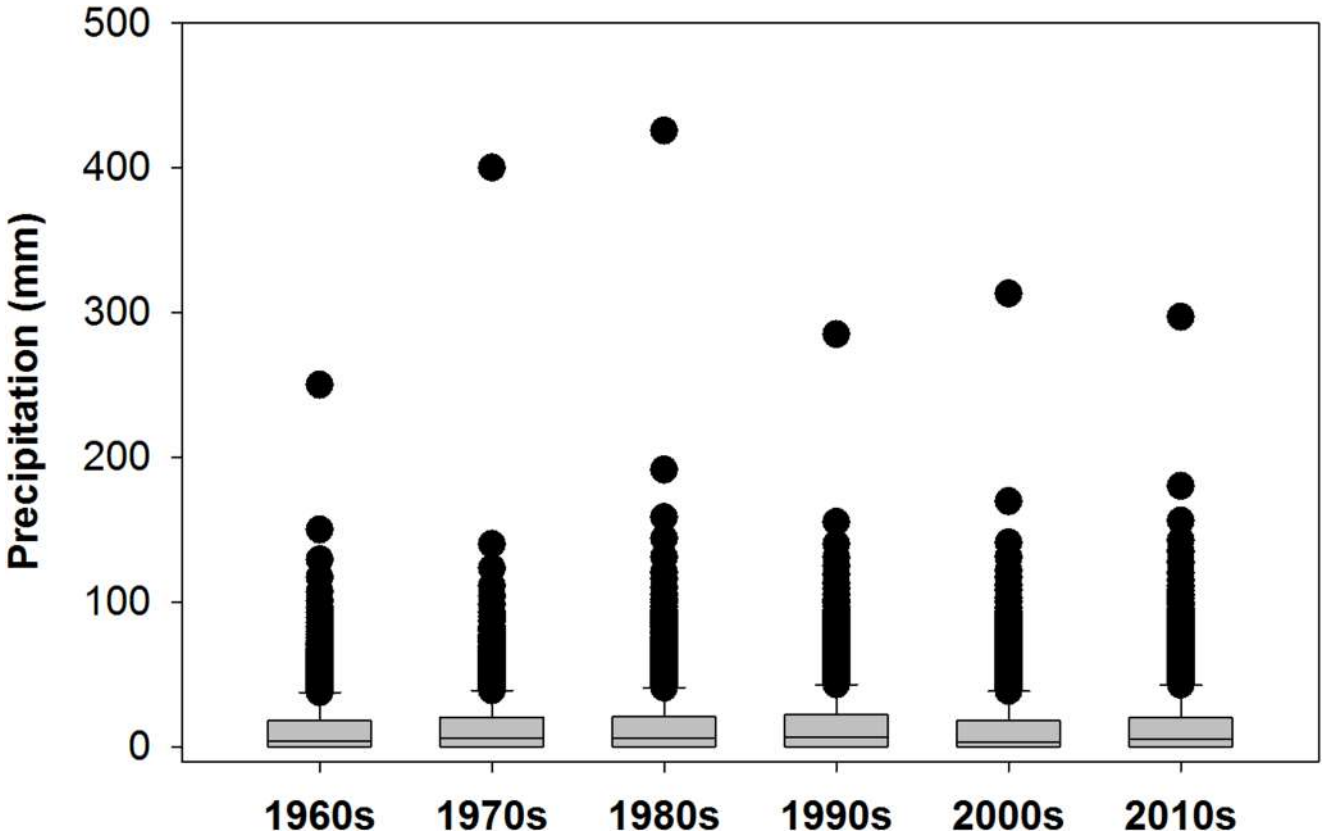

Fig. 3 Boxplots showing the precipitation recorded during the extreme precipitation days in all the meteorological stations per decade

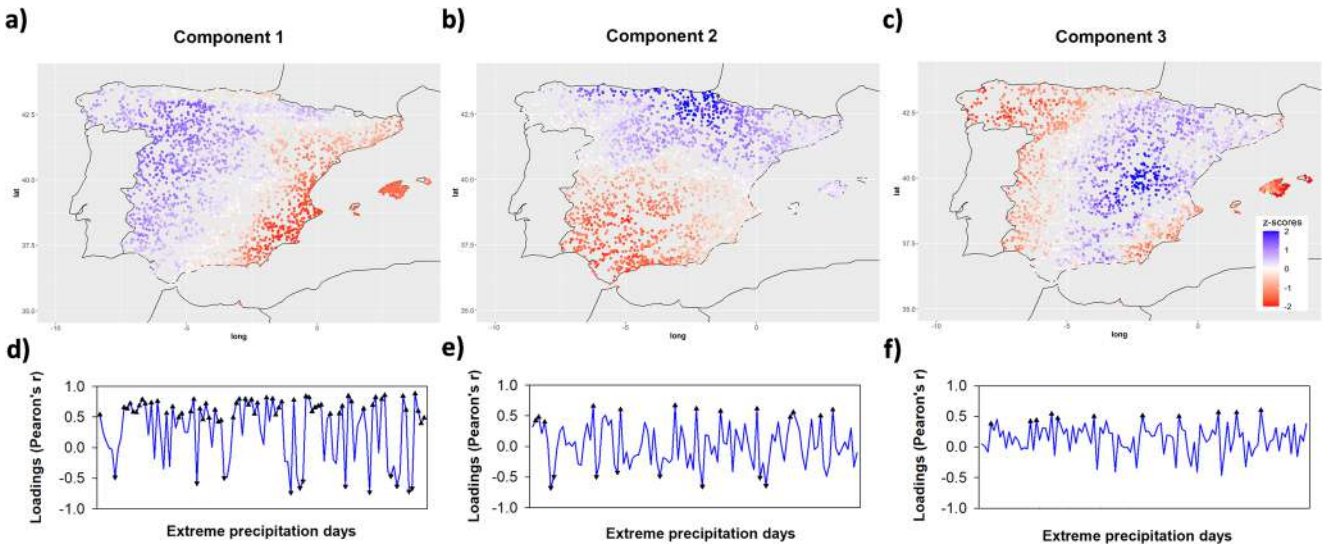

Fig. 4 Top: Spatial distribution of the three first standardized components selected (**a**, **b**, **c**) from the patterns recorded during the extreme precipitation days. Bottom: Temporal evolution of the loadings corresponding to each component (**d**, **e**, **f**), indicating those days that are representative of each one of the components. Positive configurations of the components are represented by a triangle and negative configurations by an inverted triangle

3.2.1 Component 1 positive

The analysis of the 60 WEPEs corresponding to the positive phase of Component 1 (characterized by high precipitation in the northwest and low precipitation in the southeast) reveals that the Z500 anomalies for these events show strong negative values (below −150 m) northwest of the Iberian Peninsula, indicative of a cyclonic circulation pattern. This Atlantic Low generates westerly flows (see arrows in Fig. 5a) that transport moisture toward Spain, creating favorable conditions for extreme precipitation. The role of the jet stream further corroborates the atmospheric circulation features associated with the positive phase of Component 1. As shown in Figs. 5c and d, the North Atlantic EDJ is both intensified and displaced southward, centering around a latitude of approximately 40ºN, just south of the Iberian Peninsula, facilitating enhanced dynamical forcing and moisture convergence over Spain. This displacement and intensification are particularly pronounced during winter (DJF) (26 cases; see Figure S5), although the overall circulation pattern is similar regardless of the season (Figure S6). Additionally, the tilt of the jet (its inclination with respect to the zonal axis) is reduced during these events as compared to the climatology (Fig. 5d), which likely contributes to prolonged and widespread precipitation by maintaining a steady inflow of moist air over the region. The spatial distribution of daily accumulated precipitation (Fig. 5b) shows the maxima across western Spain, including both the northwest and southwest regions, indicating the widespread nature of these events. Interestingly, the areas with the largest IVT (Fig. 5e) and TCWV (Fig. 5g) anomalies, located over the southwestern Iberian Peninsula, do not coincide with the regions of stronger atmospheric instability, which are instead concentrated over the northwest (Fig. 5f). The spatial distribution of daily accumulated precipitation (Fig. 5b) aligns more closely with the IVT and TCWV anomalies, suggesting that enhanced moisture convergence and advection play a more critical role than instability in driving the EPEs.

Figure 5h–i provides additional insights into the sources of moisture transport. Days characterized by the positive phase of Component 1 reveal anomalies in regional moisture sources. Specifically, the primary source of atmospheric moisture is located over the Atlantic Ocean, west of the Iberian Peninsula and east of the Azores, as well as over continental areas in southern Iberia. Notably, positive anomalies in E-P appear in the moisture contribution from the oceanic region west of Iberia, while negative anomalies emerge in moisture sources from the continental sources (the inner Iberian Peninsula). These moisture anomalies are consistent with the defined cyclonic circulation patterns and their associated westerly flows, confirming the key role of the Atlantic Ocean as the primary moisture source for these WPESs. As the air masses travel over the Atlantic, they become increasingly moisture-laden before reaching the Iberian Peninsula. This moisture uptake explains why the difference between evaporation and precipitation (E–P) is negative along their trajectory over these Atlantic regions.

Fig. 5 **a** Anomalies of geopotential height at 500 hPa (m) for EPEs characterized by the positive phase of Component 1, relative to the 1981–2010 climatology. The arrows represent the anomalies of horizontal wind at 850 hPa. Anomalies are only shown when they are statistically significant at the 95% (determined through a 1000-trial bootstrap resampling method). **b** Mean daily accumulated precipitation for EPEs associated with the positive phase of Component 1. **c** Anomalies in the occurrence of the North Atlantic EDJ (%) for the EPEs associated with the positive phase of Component 1, relative to the 1981–2010 climatology. **d** Distribution of the EDJ parameters (Intensity [m per s], Central Latitude [°N], Eastward Extension [°E], Tilt [°N/60°E]) for EPEs associated with the positive phase of Component 1 (left) and the 1981–2010 climatological period (right). The boxes extend from the first quartile (Q1) to the third quartile (Q3) of the data, with a horizontal line indicating the median. Whiskers extend up to 1.5 times the IQR, **e** anomalies in IVT (Integrated Vapor Transport), **f** anomalies in atmospheric instability (measured as -omega, where positive values indicate upward vertical motion), **g** anomalies in TCWV (Total Column Water Vapor, also known as IWV—Integrated Water Vapor or precipitable water), **h** Integrated moisture source pattern between 1 and 10 days backward in time mode before the day of the EPEs corresponding to the events represented by the Component 1 (Positive), (i) E-P anomalies regarding the long-term average

3.2.2 Component 1 negative

While 60 cases were identified for Component 1 Positive, the number of events is reduced for Component 1 Negative, with only 12 cases, suggesting that this precipitation pattern can arise under more unusual synoptic configurations or may not depend strongly on large-scale circulation but rather on mesoscale atmospheric processes, such as convection and atmospheric instability, as discussed later. This interpretation is supported by the seasonal distribution of the events, with the majority (8) occurring between September and November, only three during winter, and one in April. The limited number of cases may partly reflect the limited sample size but the Z500 anomalies associated with Component 1 Negative (Fig. 6a and Fig. S6) show a positive anomaly center over northern Europe (blocking high), accompanied by a negative anomaly center over Morocco. This cyclonic system south of Spain generates an airflow that brings dry air from North Africa into Spain from the east and southeast (Fig. 6a). As this flow originates predominantly from the east, the EDJ plays a minor role during these events, being displaced poleward over Europe, further north of the positive Z500 anomalies (Fig. 6c and d).

The spatial distribution of daily accumulated precipitation (Fig. 6b) shows the highest precipitation accumulation over eastern Iberia, consistent with the characteristic pattern of Component 1 Negative and the observed easterly to

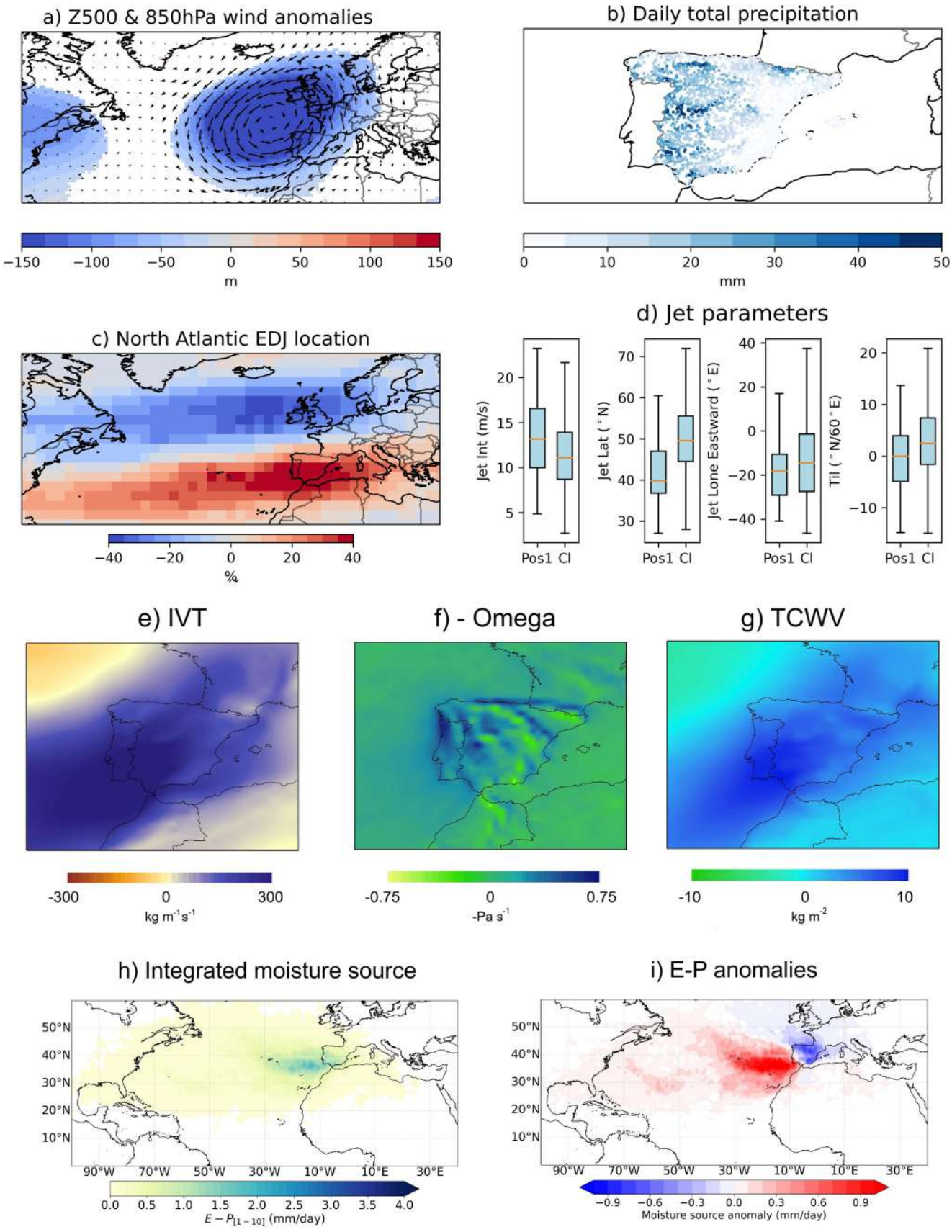
a) Z500 & 850hPa wind anomalies
−150 −100 −50 0 50 100 150
m
b) Daily total precipitation
0 10 20 30 40 50
mm
c) North Atlantic EDJ location
−40 −20 0 20 40
%
d) Jet parameters
Jet Int (m/s)
Jet Lat (° N)
Jet Lone Eastward (° E)
Til (° N/60° E)
Pos1 Cl
e) IVT
-300 0 300
kg m-1s-1
f) - Omega
-0.75 0 0.75
-Pa s-1
g) TCWV
-10 0 10
kg m-2
h) Integrated moisture source
50°N 40°N 30°N 20°N 10°N
90°W 70°W 50°W 30°W 10°W 10°E 30°E
0.0 0.5 1.0 1.5 2.0 2.5 3.0 3.5 4.0
E − P[1 − 10] (mm/day)
i) E-P anomalies
−0.9 −0.6 −0.3 0.0 0.3 0.6 0.9
Moisture source anomaly (mm/day)

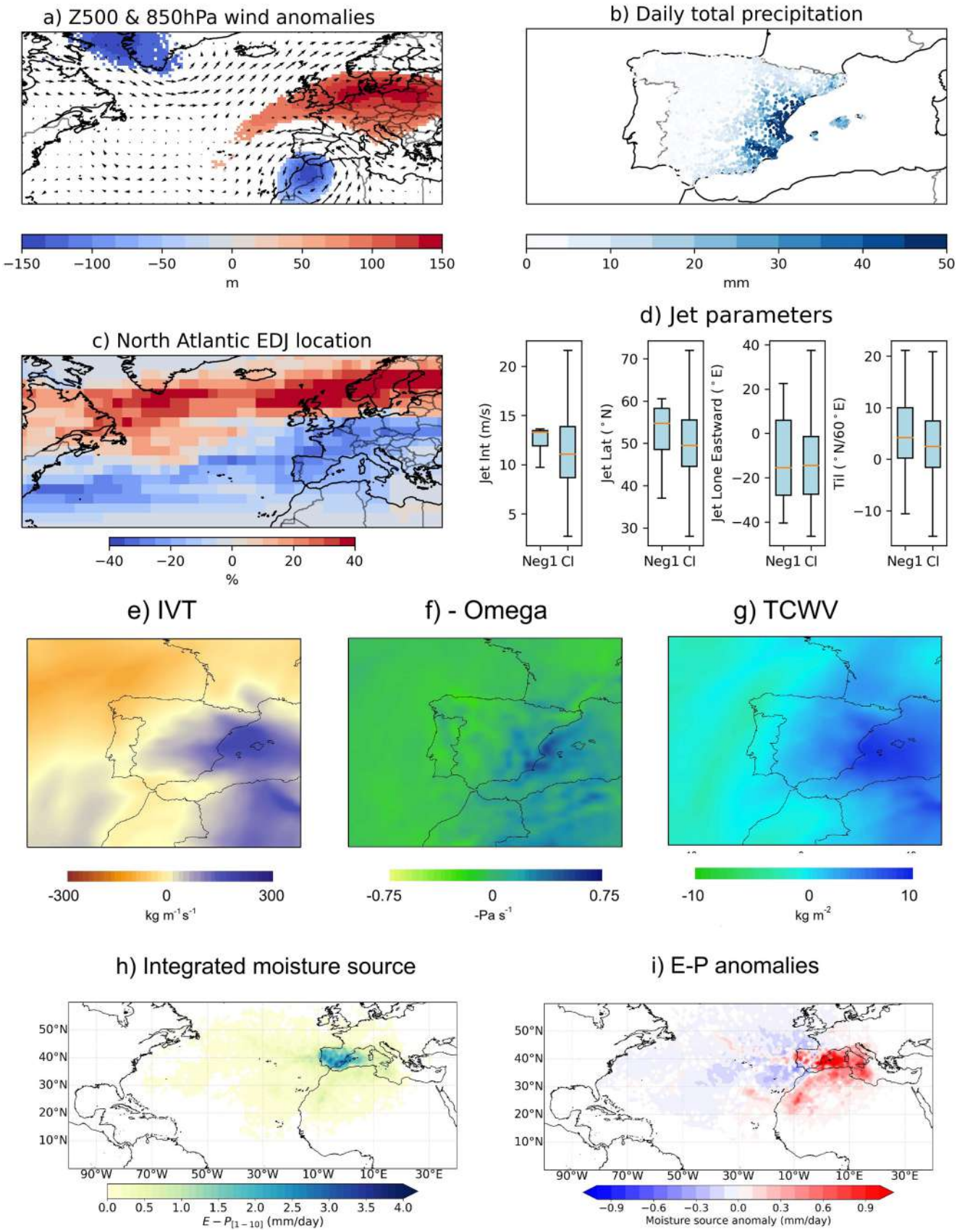

Fig. 6 As Fig. 5 but for the Component 1 (Negative)

southeasterly wind flows (Fig. 6a). The moisture transport (Fig. 6e), total column water vapor (Fig. 6g), and vertical motion (Fig. 6f) during these days exhibit a localized component, primarily confined to the eastern part of the Iberian Peninsula, where high precipitation amount is recorded during these WEPEs. Unlike the positive phase of Component 1, in this case, atmospheric instability aligns spatially with the regions of maximum precipitation (compare Fig. 6b and f). Notably, the highest instability values are located over the Mediterranean Sea, just off the eastern coast of Iberia (Fig. 6f), highlighting the important role of the Mediterranean of both moisture and energy source in triggering these WEPEs. These convective processes, characterized by local and regional scale, help to explain the absence of a dominant large-scale WR associated with Component 1 Negative. Together with the atmospheric stability, these days are also characterized by significant humidity transport and elevated water vapor throughout the entire atmospheric column (Fig. 6e, g), aligning closely with the moisture source associated with the negative phase of Component 1, which is dominated by high evaporation-minus-precipitation (E-P) values over the Iberian Peninsula and the western Mediterranean. Positive anomalies appear across this area, extending to western Sahara, while negative anomalies are observed over the Atlantic west of Iberia (Fig. 6h–i).

All these characteristics—the Z500 anomaly configuration, with a positive anomaly over northern Europe and an isolated cyclonic anomaly over Morocco; the prevailing easterly to southeasterly wind flow; the spatial pattern of precipitation concentrated over eastern Iberia; and the role of atmospheric instability in triggering precipitation—suggest that Component 1 Negative is frequently associated with cut-off lows. These systems are typically characterized by an upper-level cyclonic anomaly detached from the main westerlies, often leading to regional-scale convective activity and heavy precipitation events, as observed here.

3.2.3 Component 2 positive

The positive phase of Component 2 has a total of 13 events, distributed across seasons as follows: 6 in autumn (SON), 4 in winter (DJF), 2 in summer (JJA), and 1 in spring (MAM). Anomalies of Z500 show significant low pressures over Spain and surrounding areas, as well as high-pressure anomalies over the North Atlantic (Fig. 7a). However, a seasonal breakdown highlights substantial spatial differences in the anomaly patterns. In autumn, the significant negative Z500 anomalies are mainly concentrated over the Iberian Peninsula. In winter, while the positive anomalies over the North Atlantic are more intense than in autumn, the negative anomalies shift northward to central and northern Europe, illustrating a different synoptic configuration (Fig. S8).

The EDJ analysis provides additional insights into atmospheric dynamics. Although the mean latitude of the jet does not deviate significantly from climatology, the tilt parameter exhibits positive anomalies. This is visible in the positive anomalies of jet occurrence west of the North Atlantic (Fig. 7c) and in the tilt distribution (Fig. 7d). These anomalies reflect the influence of the high-pressure systems over the North Atlantic, which favor a wavier jet configuration than the climatology. This wavy jet pattern causes northerly winds to dominate over Spain, with a particularly strong influence over the northern region (see jet occurrence anomalies in Fig. 7c as well as the EDJ eastward extension distributions in Fig. 7d).

The precipitation observed during these events is concentrated over northern Spain (Fig. 7b), which aligns with the characteristic pattern for the positive phase of Component 2. The IVT anomaly map displays predominantly positive values across the Iberian Peninsula, with a clear indication of moisture transport from the North Atlantic towards the Mediterranean (Fig. 7e), consistent with the atmospheric circulation pattern and jet characteristics discussed earlier. In contrast, atmospheric instability is particularly intense over the Pyrenees and southeastern Iberia (Fig. 7f), though these regions differ in their association with precipitation. TCWV also shows predominantly positive anomalies but is mainly confined to northeastern Iberia (Fig. 7g). This combination of water vapor presence and atmospheric instability over the Pyrenees leads to WEPEs in this region, whereas the southeast, despite high instability, experiences little precipitation due to limited water vapor availability. Overall, the precipitation in northern Iberia, characteristic of the positive phase of Component 2, can be attributed to distinct mechanisms: in the western part, it is primarily driven by moisture advection, while in the eastern Pyrenees, orographic influences and strong instability also play a critical role. During these WEPEs, humidity primarily originates from southern and eastern Iberia, as well as Mediterranean areas near the coast, and to a lesser extent from the North Atlantic (Fig. 7h–i). The moisture contribution from southern and eastern Spain results from cyclonic circulation associated with the significant negative anomalies over this region, as shown in the wind flow in Fig. 7a. Conversely, the moisture originating from the North Atlantic is transported by the wavy jet surrounding the significant positive anomalies (visible in the wind flows in Fig. 7a and the precipitation trace in Fig. 7b). These combined moisture sources enhance moisture convergence and precipitation over northern Spain.

3.2.4 Component 2 negative

The negative phase of Component 2 encompasses eight cases, evenly distributed between winter (4) and autumn

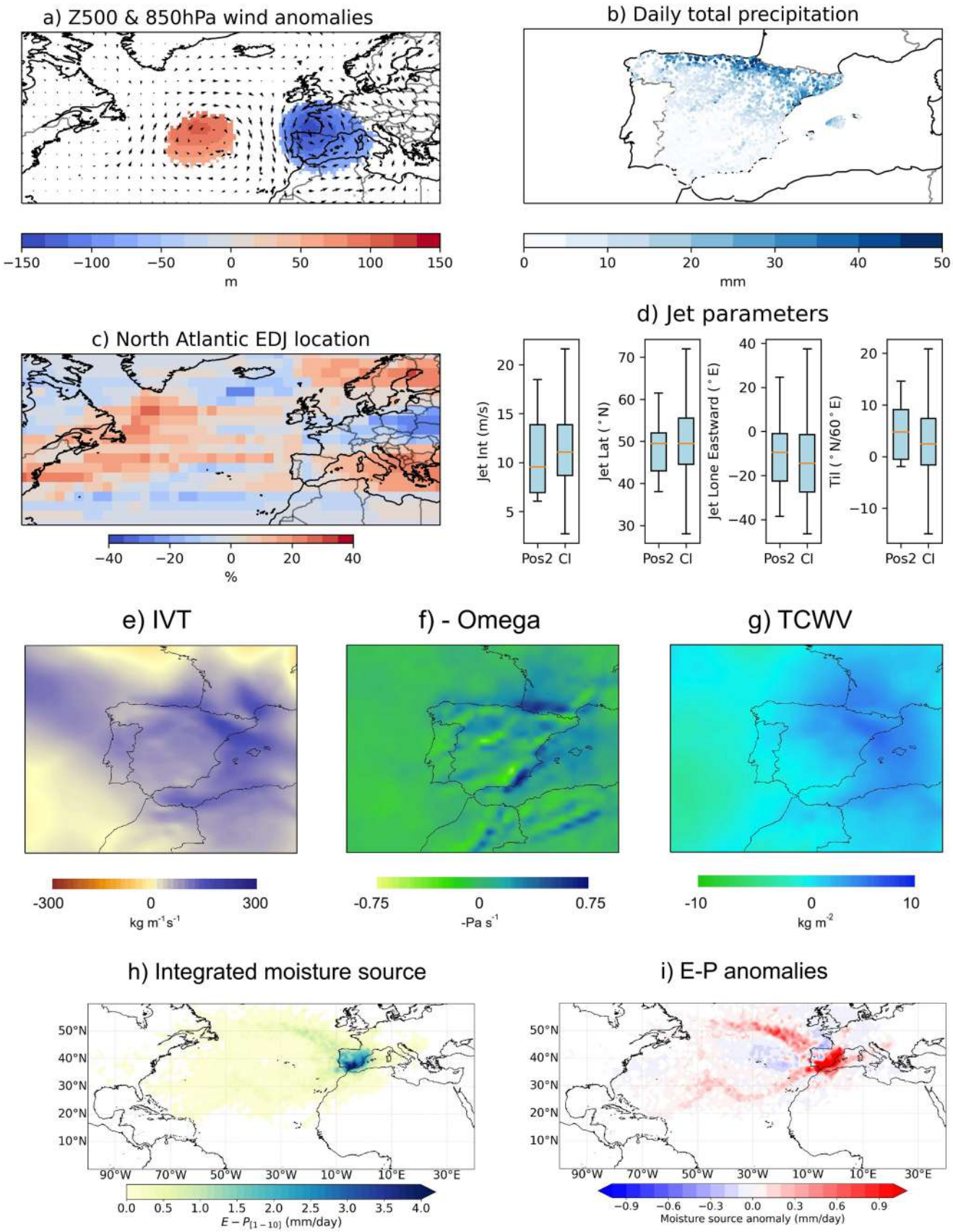

Fig. 7 As Fig. 5 but for the Component 2 (Positive)

(4). In winter, a high-latitude blocking pattern is evident to the east of Greenland, accompanied by strong negative Z500 anomalies extending from the Azores region to central Europe (Fig. S9). These anomalies are associated with a highly zonal and southward-displaced jet stream, located around 30°N with small tilt (Fig. 8c and d). In contrast, during autumn, positive Z500 anomalies are observed at mid-latitudes, west of the United Kingdom, while the negative anomalies are less extensive and more localized than in winter (Figure S10). This low-pressure system seems to be detached from the general circulation (similar as a cut-off low) and tends to be located southwest of Iberia.

Precipitation during these WEPEs is mainly concentrated over southern Iberia (Fig. 8b), in agreement with the characteristic pattern of the negative phase of Component 2. In both winter (due to the southward-shifted jet) and autumn (due to the detached low-pressure system southwest of Iberia), the synoptic conditions drive southerly/southwesterly winds toward Spain (Fig. S8). Consequently, moisture is transported from both the Atlantic toward southern Spain (Fig. 8h-i), supporting the observed precipitation patterns. The moisture transport (Fig. 8e) and total column water vapor (Fig. 8g) anomalies are distinctly positive in the southern Iberian Peninsula. Additionally, there is significant vertical air motion in this region (Fig. 8f), which likely contributes to destabilizing the abundant water vapor available and generating heavy precipitation in southern Spain during these WEPEs.

3.2.5 Component 3 positive

The positive phase of Component 3 includes 11 cases, distributed across autumn (5), spring (4), winter (1), and summer (1). This type of WEPE is characterized by precipitation concentrated along a longitudinal band in central Spain, leaving the western and southeastern regions with little to no rainfall. This pattern aligns well with the precipitation observed on the days classified under this component (Fig. 9b).

The associated atmospheric circulation resembles that described for the positive phase of Component 2, with a low-pressure system over Iberia and positive Z500 anomalies over the North Atlantic (Fig. 9a). However, key differences emerge upon closer examination. While both components exhibit a dipolar structure, the positive anomalies over the Atlantic in Component 3 are weaker and barely significant, whereas the negative anomalies over Iberia are more intense and extend over a broader region compared to Component 2 (compare Figs. 7 and 9). Another major distinction lies in the position of the Z500 anomaly minimum, which strongly influences the prevailing wind patterns over Iberia. In Component 2, the centre of negative anomalies is located slightly north of Iberia, resulting in a cyclonic flow dominated by northerly or northwesterly winds, as previously discussed (Fig. 7a). In contrast, for Component 3, the Z500 anomaly minimum shifts westward, near Portugal, leading to a counterclockwise circulation and a predominantly southerly flow over Iberia (Fig. 9a). This flow transports moisture from the North Atlantic adjacent to Portugal, producing rainfall over much of Spain, except for the westernmost areas (Fig. 9b).

The IVT anomalies align well with the identified moisture sources in Fig. 9h-i and the atmospheric circulation pattern depicted in Fig. 9a, showing positive anomalies across central, southern, and eastern Iberia (Fig. 9e). This results in a substantial amount of water vapor in the central and eastern parts of the peninsula (Fig. 9g). However, WEPEs predominantly occur along the central longitudinal band due to higher atmospheric instability compared to the western regions (Fig. 9f).

Seasonal differences for this component are small, though the anomalies in spring are less intense and shifted further south compared to those in autumn (Fig. S11). Furthermore, the SON configuration can promote the advection of cold air in the mid and upper troposphere from northern Europe towards the Iberian Peninsula. This interaction between the colder air aloft and the warm, moist air near the surface over central Iberia increases the vertical temperature gradient, enhancing atmospheric instability and favouring convection. Additionally, the positive Z500 anomalies over the North Atlantic prevent the jet stream from shifting southward, reducing its influence on precipitation in Spain (Fig. 9c and d).

4 Discussion

4.1 Trends in WEPEs

This study has analyzed WEPEs affecting widespread areas of Spain, utilizing a high-density network of daily precipitation records. By identifying the most WEPEs, this approach advances beyond previous analyses that rely on isolated stations, individual events, or gridded datasets. Our approach allows for robust examination of the trends in the frequency and magnitude of extreme events without the limitations of spatial randomness that affect the low number of very extreme events that are typically the case for many meteorological databases (García-Ruiz et al. 2000; Ribes et al. 2019).

We have shown that WEPEs have not exhibited a trend in either frequency or magnitude since 1961. This finding aligns with previous observations based on gridded data and meteorological observatory series. Although some studies suggest an increase in annual maximum precipitation

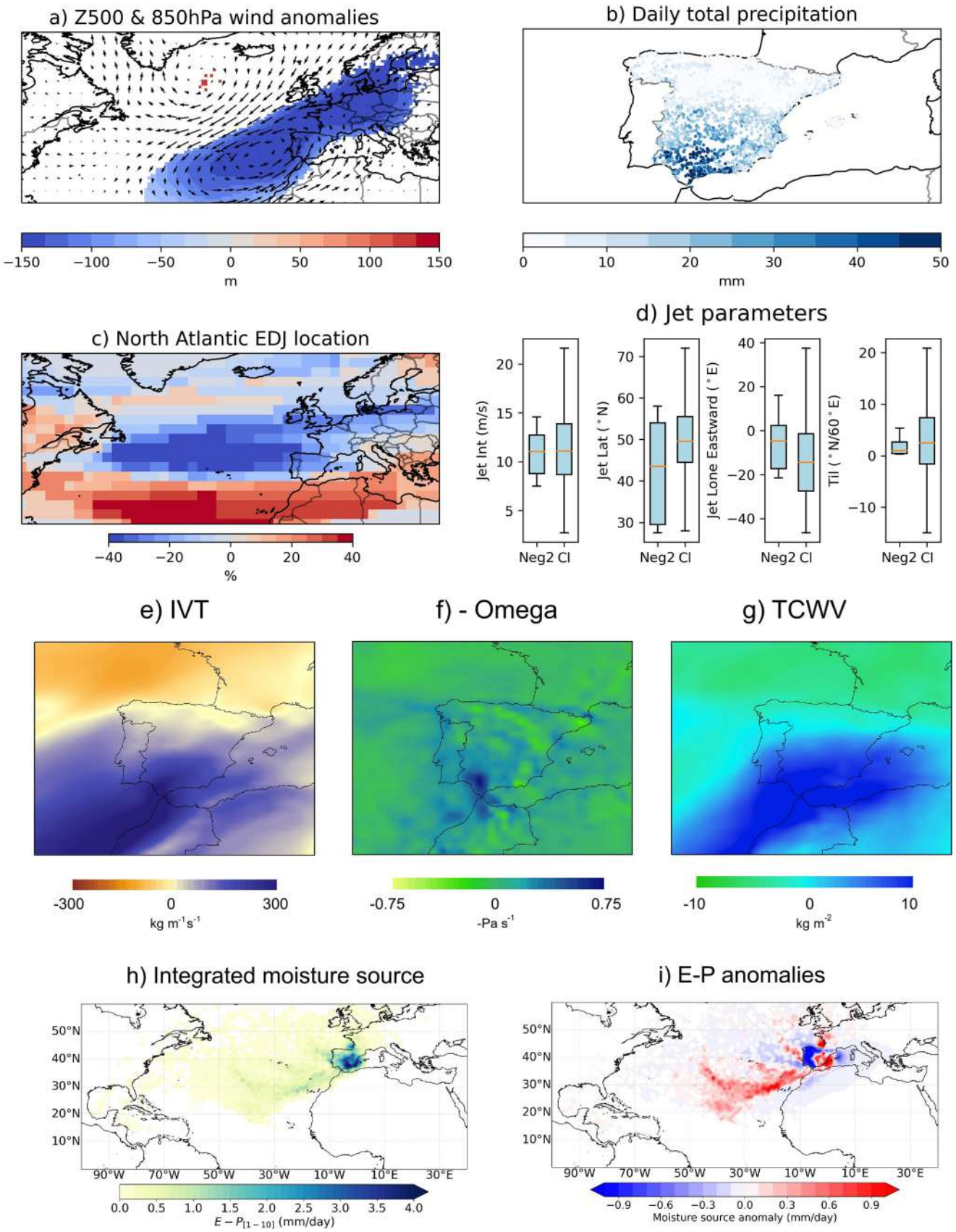

Fig. 8 As Fig. 5 but for the Component 2 (Negative)

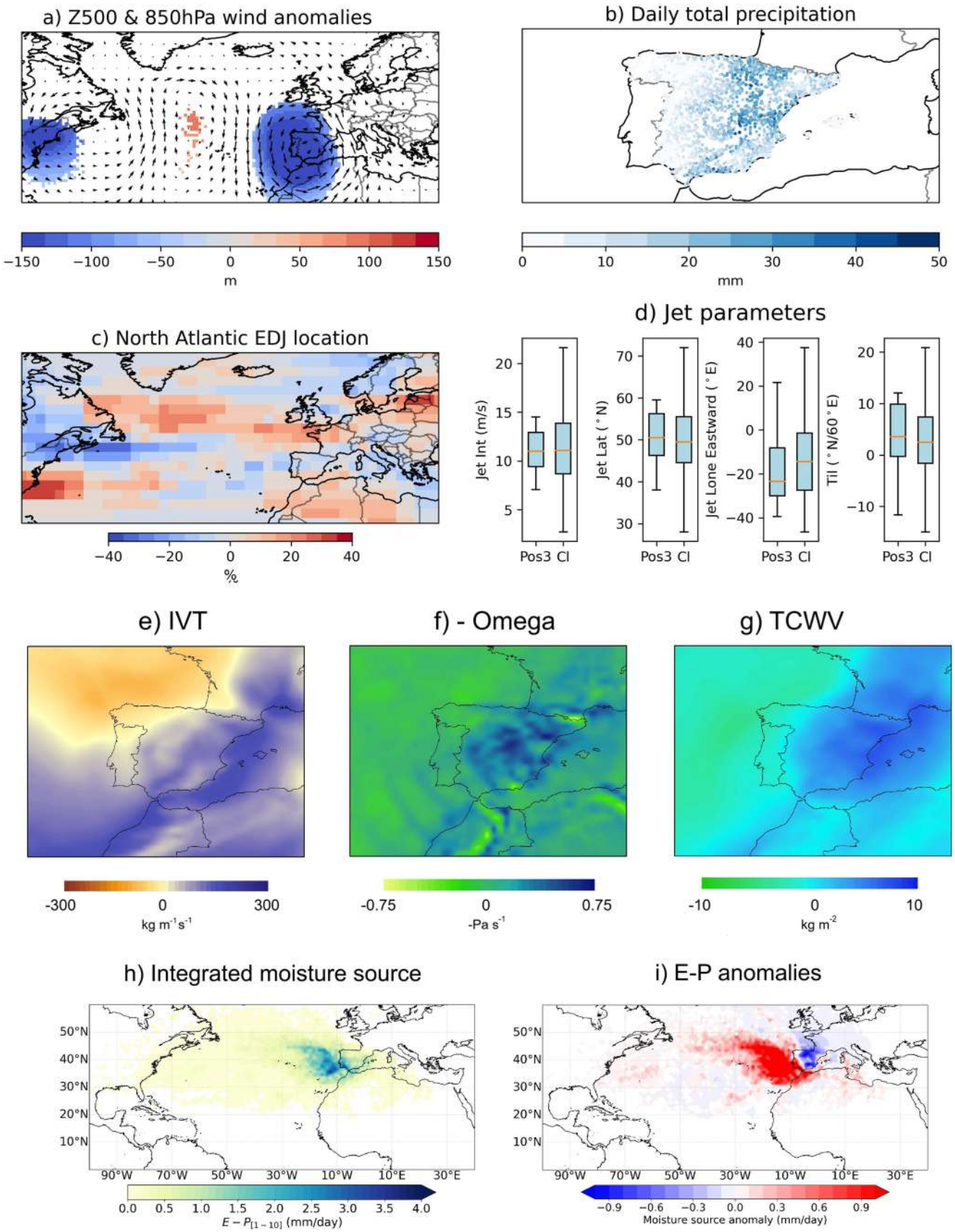

Fig. 9 As Fig. 5 but for the Component 3 (Positive)

over significant parts of Spain, especially in the colder seasons (Senent-Aparicio et al. 2023), the majority of existing research supports a stationary behavior in extreme precipitation (Beguería et al. 2011; Gallego et al. 2011; Serrano-Notivoli et al. 2018). While this does not preclude the possibility of increased maximum intensity of specific regional events, such as in eastern Spain and in the Mediterranean coastland (Acero et al. 2011; Miró et al. 2022; Senent-Aparicio et al. 2023), WEPEs do not show this trend.

There is currently significant uncertainty regarding potential changes in WEPEs, linked to atmospheric circulation, convection, and stratification (Fowler et al. 2021). Some global studies indicate that WEPEs may be increasing, mainly due to thermodynamic mechanisms associated with climate change (Donat et al. 2013b; Seneviratne et al. 2021), with these mechanisms expected to drive projected increases in extreme precipitation globally (O'Gorman 2015; Pfahl et al. 2017) and in Spain (Requena et al. 2023). However, while the influence of thermodynamic mechanisms is plausible, several factors could explain the lack of an increasing trend in the frequency or magnitude of WEPEs in Spain over the last decades. One primary factor is that these events are mostly recorded during winter months, when atmospheric dynamics play a dominant role, diminishing the relevance of thermodynamic mechanisms. For example, extratropical storms, characterised by strong 500 hPa negative anomalies in western Europe, do not show a clear trend in their frequency or severity (Seneviratne et al. 2021), particularly in the Mediterranean region (Sousa et al. 2021).

In contrast, at the end of the summer season when thermodynamic mechanisms may be more significant (e.g., enhancing convection favoured by high sea surface temperature), an increase in the intensity of WEPEs could be more plausible related with cut-off lows, which are a common synoptic feature over Iberia, particularly in the western Mediterranean, where they play a key role in extreme precipitation episodes (Nieto et al. 2005). Nevertheless, these events are more local (Romero et al. 1997; Homar et al. 2002), and they are not well identified with the methodology used here to characterise WEPEs. In any case, in the last two decades we have observed an increase in frequency of the spatial configuration associated with the negative component 1, which corresponds to eastern Spain, which could suggest an enhanced influence of cut-off lows and high sea surface temperatures in the Mediterranean (Nieto et al. 2005; Awan and Formayer 2017; Muñoz et al. 2020).

4.2 Spatial patterns of WEPEs

A key conclusion of our study is the coherent spatial structure of WEPEs in Spain, which exhibit well-defined patterns that allow many of these events to be categorized into a few distinct types. Understanding these patterns is particularly important for assessing potential widespread hydrological impacts, given the cumulative flow effects when large areas experience extreme precipitation. Additionally, regional studies in Spain have highlighted significant spatial differences in WEPE characteristics. For example, variations between eastern and western Andalucía are documented (Hidalgo-Muñoz et al. 2011), but also in Catalonia (Martínez et al. 2007) and the Ebro basin (Vicente-Serrano et al. 2009), in line with the results by (Queralt et al. 2009), who showed that atmospheric circulation mechanisms as the North Atlantic Oscillation exerts a clear effect on the intensity of extreme precipitation rates in northern and westernmost Spanish regions, whereas in central and southwestern areas this mechanisms is only affecting the frequency of precipitation, particularly in winter (Merino et al. 2016). These previous results reinforce one of the main findings of our study: the important spatial differences across Spain in the development of WEPEs, which would be associated with different dynamic mechanisms.

4.3 Atmospheric mechanisms determining the WEPEs Spatial configurations

The classification of WEPEs in Spain identifies five distinct atmospheric circulation patterns, each characterized by specific synoptic configurations and moisture transport mechanisms: (i) Atlantic Low Pattern (positive Component 1)—This pattern is associated with a low-pressure system over the North Atlantic, which enhances strong westerly flows and widespread precipitation over northern and western Iberia, (ii) Cut-off Low Pattern (negative Component 1)—This pattern corresponds to isolated low-pressure systems detached from the main westerly flow, leading to localized but intense precipitation, primarily in eastern Spain, (iii) Latitudinal Dipole Pattern (positive Component 2)—Characterized by an Iberian Low and an Atlantic Block High, this pattern induces a cyclonic circulation centered over Iberia, generating northwesterly or westerly flows that transport moisture and favor precipitation in northern and central Spain, (iv) Southern Mixed Regime (negative Component 2)—This pattern varies seasonally: in autumn, precipitation is dominated by a cut-off low southwest of Iberia, while in winter, a zonally elongated low-pressure system, associated with a displaced jet stream, leads to intense precipitation over southern Spain, and (v) Iberian Low Pattern (positive Component 3)—This pattern features a deep low-pressure anomaly over Iberia, accompanied by a weak but significant high-pressure anomaly over the Atlantic. This configuration enhances southerly moisture transport from

the North Atlantic near Portugal, concentrating precipitation in a central longitudinal band across Spain.

These findings highlight the diversity of circulation regimes driving WEPEs in Iberia and emphasize the importance of both large-scale and regional-scale dynamics in shaping their spatial distribution. Furthermore, some of these configurations align with atmospheric circulation anomalies that influence precipitation over large areas of the North Atlantic, in agreement with previous studies. For instance, Kautz et al. (2022) observed that in Europe, blocking conditions can lead to extreme precipitation by inducing meridional advection of air masses to the south and shifting storm tracks—patterns consistent with those observed in positive Component 1 and negative Component 2.

Other spatial configurations are characteristic of more regional atmospheric conditions. For example, during the cut-off low pattern characteristic of the negative Component 2, there are no influences of the intensity and position of the Polar Jet Stream, but regional moisture transport, water vapor availability, and vertical air motion create favourable conditions for heavy precipitation. This is particularly evident in the spatial configuration characteristic of high precipitation in the southern and eastern regions of Spain. In this sense, Pérez-Zanón et al. (2018) analyzed long-term extreme events in southern Catalonia, highlighting that severe convective events often coincide with low-pressure systems, cold fronts, and temperature anomalies due to the temperature contrast between the lower and mid-troposphere and the humidity contribution from lower atmospheric levels. Similarly, Romero et al. (1999b) identified several atmospheric circulation drivers influencing torrential precipitation events along the Mediterranean coast, with the position of 500 hPa anomalies, with differential influences of the Atlantic and Mediterranean disturbances.

4.4 The role of the jet-stream anomalies

For the first time, we have examined the role of jet stream anomalies on WEPEs in Spain. Such jet stream anomalies and associated Rossby wave undulations are considered key factors in extreme European events (Huntingford et al. 2019), potentially intensified by Arctic amplification and enhanced wave undulations due to the current warming (Kornhuber et al. 2020). This mechanism may underpin hypotheses about the increasing role of cut-off lows and high-convection systems in southern Europe and North Africa (Greco et al. 2020; Grazzini et al. 2021; Llasat et al. 2021). In Spain, we have demonstrated that southward displacements of the Polar Jet Stream lead to widespread precipitation events in western Spain, while northward shifts are associated with events in the Mediterranean region (negative Component 1). The latter situation promotes the formation of low pressure systems centered over North Africa. These systems, in turn, generate easterly flows towards the Iberian Peninsula—a pattern well-documented in prior studies (Homar et al. 2002; Rigo and Llasat 2004; Awan and Formayer 2017), which promotes vertical air motion that interacts with the region's topography, further intensifying the effects (Romero et al. 1997; Peñarrocha et al. 2002; Mastrantonas et al. 2021).

4.5 The influence of the moisture source anomalies

Our findings also reveal notable moisture source anomalies compared to average conditions on days with WEPEs. Anomalous moisture transport from different sources has been suggested as a key factor in WEPEs, often associated with regional-scale phenomena such as atmospheric rivers (Eiras-Barca et al. 2018; Ramos et al. 2018; Huang et al. 2020; Yokoyama et al. 2020; Gimeno-Sotelo and Gimeno 2023) and low-level jets (Liu et al. 2020). However, our findings indicate that WEPEs in Spain can also be linked to local anomalies in moisture sources over the continental Iberian Peninsula and surrounding oceanic areas, particularly the Mediterranean Sea, when compared to average moisture sources for Spanish precipitation (Gimeno et al. 2010). Significant differences exist in moisture source anomalies between widespread precipitation events affecting the eastern Mediterranean coast, where anomalies over the Mediterranean are particularly influential, and events in western Spain, where a high supply of anomalous humidity from the Atlantic Ocean is critical. Previous research has also emphasized the crucial role of the Mediterranean aea, with positive sea surface temperature anomalies identified as key drivers of these events (Pastor et al. 2001). We have not analysed the role of the sea surface temperature on these events. Nevertheless, we have demonstrated that the western Mediterranean region supplies a significant amount of the moisture driving precipitation during the events characterised by a *Cut-off Low* pattern (negative Component 1). These influences underscore the importance of coupled atmospheric-sea conditions in generating extreme precipitation (Romero et al. 1999b; Ramis et al. 2013), consistent with a large atmospheric vertical air motion as observed in our study.

4.6 Future implications

Looking ahead, global climate projections suggest that warming could lead to more frequent and severe EPEs, primarily through thermodynamic processes that increase atmospheric moisture content. In Spain, studies indicate a rise in EPEs (Garijo and Mediero 2019), particularly during warmer months when thermodynamic mechanisms are more active (Requena et al. 2023). However, WEPEs in Spain

predominantly occur in winter, driven primarily by dynamic factors such as synoptic circulation patterns and jet stream configurations, as demonstrated in our study. Therefore, caution is required when assessing potential future trends of WEPEs under warming scenarios. For localized convective extreme events in eastern Spain, however, an upward trend appears plausible (Miró et al. 2022). Warmer Mediterranean sea temperatures may enhance moisture availability, fueling higher-intensity events in this region. Thus, this study underscores the importance of distinguishing between widespread and localized extreme events, as future changes will likely depend on both global climate thermodynamic influences and specific regional atmospheric dynamics.

5 Conclusions

Our study demonstrates that widespread extreme precipitation events in Spain have not exhibited a clear trend and significant in either frequency or magnitude since 1961, aligning with previous research based on gridded datasets and station-based precipitation series. Our results also highlight the spatial heterogeneity of WEPEs across Spain, emphasizing the role of distinct atmospheric circulation patterns in shaping their distribution. The classification of five major circulation patterns reveals that different regions experience WEPEs under varying synoptic conditions, with some mechanisms—such as cut-off lows—being more influential in eastern and southern Spain. These findings reinforce the importance of regional-scale dynamics, including moisture transport and vertical air motion, in determining extreme precipitation events. Nevertheless, WEPEs in Spain are primarily governed by dynamic drivers such as jet stream anomalies and synoptic circulation patterns. Future research should further investigate how these processes interact to refine projections of extreme precipitation under changing climate conditions.

Supplementary Information The online version contains supplementary material available at https://doi.org/10.1007/s00382-025-07829-y.

Acknowledgements This work has been supported by the research projects TED2021-129152B-C41 and PID2022-137244OB-I00, financed by the Spanish Ministry of Science and FEDER, and MEHYDRO (LINKB20080) financed by the i-LINK 2021 programme by CSIC, CSIC's Interdisciplinary Thematic Platform Clima (PTI-Clima) and contract CSC2023-02-00 financed by the Ministry for the Ecological Transition and the Demographic Challenge (MITECO) and the European Commission NextGenerationEU (Regulation EU 2020/2094). José C. Fernández-Alvarez acknowledges the support from the postdoctoral contract funded by the Xunta de Galicia under grant IN606B-2024.16. EPhysLab members were supported by the following projects: PID2021-122314OB-I00 and TED2021-129152B-C43, funded by the Ministerio de Ciencia, Innovación y Universidades, Spain (MICIU/AEI/https://doi.org/10.13039/501100011033), Xunta de Galicia (grant ED431C2021/44; Programa de Consolidación e Estructuración de Unidades de Investigación Competitivas (Grupos de Referencia Competitiva), Consellería de Cultura, Educación e Universidade) and the European Commission 'ERDF A way of making Europe' program and "NextGenerationEU"/PRTR. The Climatoc-Lab was also supported by the RED-CLIMA 2 project funded by CSIC (Ref. LINCG24042) and the PROMETEO Grant CIPROM/2023/38 for Excellence Research Groups funded by the GVA. This work by Luis Gimeno-Sotelo is partially financed by national funds through FCT – Fundação para a Ciência e a Tecnologia under the project UIDB/00006/2020, https://doi.org/10.54499/UIDB/00006/2020, and project UID/00006/2025.

Funding Open Access funding provided thanks to the CRUE-CSIC agreement with Springer Nature.

Data availability The data that support the findings of this study are available from the corresponding author upon reasonable request.

Declarations

Conflict of interest The authors declare no competing interests.

References

Acero FJ, García JA, Gallego MC (2011) Peaks-over-threshold study of trends in extreme rainfall over the Iberian Peninsula. J Clim 24:1089–1105. https://doi.org/10.1175/2010JCLI3627.1

Alexander LV, Bador M, Roca R et al (2020) Intercomparison of annual precipitation indices and extremes over global land areas from in situ, space-based and reanalysis products. Environ Res Lett 15:055002. https://doi.org/10.1088/1748-9326/ab79e2

Awan NK, Formayer H (2017) Cutoff low systems and their relevance to large-scale extreme precipitation in the European alps. Theoret Appl Climatol 129:149–158. https://doi.org/10.1007/s00704-016-1767-0

Barriopedro D, Ayarzagüena B, García-Burgos M, García-Herrera R (2023) A multi-parametric perspective of the North Atlantic eddy-driven jet. Clim Dyn 61:375–397. https://doi.org/10.1007/s00382-022-06574-w

Beguería S, Angulo-Martínez M, Vicente-Serrano SM et al (2011) Assessing trends in extreme precipitation events intensity and magnitude using non-stationary peaks-over-threshold analysis: a case study in Northeast Spain from 1930 to 2006. Int J Climatol 31:2102–2114. https://doi.org/10.1002/joc.2218

Beguería S, Tomas-Burguera M, Serrano-Notivoli R et al (2019) Gap filling of monthly temperature data and its effect on climatic variability and trends. J Clim 32:7797–7821. https://doi.org/10.1175/JCLI-D-19-0244.1

Byrne MP, O'Gorman PA (2018) Trends in continental temperature and humidity directly linked to ocean warming. Proc Natl Acad Sci USA 115:4863–4868. https://doi.org/10.1073/pnas.1722312115

Camarasa-Belmonte AM, Rubio M, Salas J (2020) Rainfall events and climate change in mediterranean environments: an alarming shift from resource to risk in Eastern Spain. Nat Hazards 103:423–445. https://doi.org/10.1007/s11069-020-03994-x

Cánovas-García F, Vargas Molina J (2024) An exploration of exposure to river flood risk in Spain using the National floodplain mapping system. Geomat Nat Hazards Risk 15:2421405. https://doi.org/10.1080/19475705.2024.2421405

Chen G, Norris J, Neelin JD et al (2019) Thermodynamic and dynamic mechanisms for hydrological cycle intensification over the full probability distribution of precipitation events. J Atmos Sci 76:497–516. https://doi.org/10.1175/JAS-D-18-0067.1

Cortès M, Llasat MC, Gilabert J et al (2018) Towards a better Understanding of the evolution of the flood risk in mediterranean urban areas: the case of Barcelona. Nat Hazards 93:39–60. https://doi.org/10.1007/s11069-017-3014-0

Cramer W, Guiot J, Fader M et al (2018) Climate change and interconnected risks to sustainable development in the mediterranean. Nat Clim Change 8:972–980. https://doi.org/10.1038/s41558-018-0299-2

Doblas-Reyes FJ, Sörensson AA, Almazroui M et al (2021) Linking global to regional climate change. Climate change 2021: the physical science basis. Contribution of working group I to the sixth assessment report of the intergovernmental panel on climate change

Donat MG, Alexander LV, Yang H et al (2013a) Global Land-Based datasets for monitoring Climatic extremes. Bull Am Meteorol Soc 94:997–1006

Donat MG, Alexander LV, Yang H et al (2013b) Updated analyses of temperature and precipitation extreme indices since the beginning of the twentieth century: the HadEX2 dataset. J Geophys Res Atmos 118:2098–2118. https://doi.org/10.1002/jgrd.50150

Eiras-Barca J, Lorenzo N, Taboada J et al (2018) On the relationship between atmospheric rivers, weather types and floods in Galicia (NW Spain). Nat Hazards Earth Syst Sci 18:1633–1645. https://doi.org/10.5194/nhess-18-1633-2018

Fernández-Alvarez JC, Pérez-Alarcón A, Nieto R, Gimeno L (2022) TROVA: transport of water vapor. SoftwareX 20:101228. https://doi.org/10.1016/j.softx.2022.101228

Ferreira RN (2021) Cut-off lows and extreme precipitation in Eastern spain: current and future climate. Atmosphere 12. https://doi.org/10.3390/atmos12070835

Fowler HJ, Ali H, Allan RP et al (2021) Towards advancing scientific knowledge of climate change impacts on short-duration rainfall extremes. Philos Trans R Soc A Math Phys Eng Sci 379. https://doi.org/10.1098/rsta.2019.0542

Gallego C, Trigo R, Vaquero J et al (2011) Trends in frequency indices of daily precipitation over the Iberian Peninsula during the last century. J Phys Res 116. https://doi.org/10.1029/2010JD014255

García-Ruiz JM, Arnáez J, White SM et al (2000) Uncertainty assessment in the prediction of extreme rainfall events: an example from the central Spanish Pyrenees. Hydrol Process 14:887–898.

Garijo C, Mediero L (2019) Assessment of changes in annual maximum precipitations in the Iberian Peninsula under climate change. Water (Switzerland) 11. https://doi.org/10.3390/w11112375

Gimeno L, Nieto R, Trigo RM et al (2010) Where does the Iberian Peninsula moisture come from? An answer based on a lagrangian approach. J Hydrometeorol 11:421–436. https://doi.org/10.1175/2009JHM1182.1

Gimeno L, Vázquez M, Eiras-Barca J et al (2020) Recent progress on the sources of continental precipitation as revealed by moisture transport analysis. Earth Sci Rev 201:103070. https://doi.org/10.1016/j.earscirev.2019.103070

Gimeno L, Eiras-Barca J, Durán-Quesada AM et al (2021) The residence time of water vapour in the atmosphere. Nat Rev Earth Environ 2:558–569. https://doi.org/10.1038/s43017-021-00181-9

Gimeno L, Sorí R, Vázquez M et al (2022) Extreme precipitation events. Wiley Interdiscip Rev Water. https://doi.org/10.1002/wat2.1611. 9:

Gimeno-Sotelo L, Gimeno L (2023) Where does the link between atmospheric moisture transport and extreme precipitation matter? Weather Clim Extremes 39:100536. https://doi.org/10.1016/j.wace.2022.100536

Gimeno-Sotelo L, Bevacqua E, Gimeno L (2023) Combinations of drivers that most favor the occurrence of daily precipitation extremes. Atmos Res 294:106959. https://doi.org/10.1016/j.atmosres.2023.106959

Grazzini F, Fragkoulidis G, Teubler F et al (2021) Extreme precipitation events over Northern italy. Part II: dynamical precursors. Q J R Meteorol Soc 147:1237–1257. https://doi.org/10.1002/qj.3969

Greco A, De Luca DL, Avolio E (2020) Heavy precipitation systems in Calabria region (southern Italy): high-resolution observed rainfall and large-scale atmospheric pattern analysis. Water (Switzerland) 12. https://doi.org/10.3390/w12051468

Hermoso A, Homar V, Amengual A (2021) The sequence of heavy precipitation and flash flooding of 12 and 13 September 2019 in Eastern spain. Part I: mesoscale diagnostic and sensitivity analysis of precipitation. J Hydrometeorol 22:1117–1138. https://doi.org/10.1175/JHM-D-20-0182.1

Hersbach H, Bell B, Berrisford P et al (2020) The ERA5 global reanalysis. Q J R Meteorol Soc 146:1999–2049. https://doi.org/10.1002/qj.3803

Hidalgo-Muñoz JM, Argüeso D, Gámiz-Fortis SR et al (2011) Trends of extreme precipitation and associated synoptic patterns over the Southern Iberian Peninsula. J Hydrol 409:497–511. https://doi.org/10.1016/j.jhydrol.2011.08.049

Homar V, Romero R, Ramis C, Alonso S (2002) Numerical study of the October 2000 torrential precipitation event over Eastern spain: analysis of the synoptic-scale stationarity. Ann Geophys 20:2047–2066. https://doi.org/10.5194/angeo-20-2047-2002

Huang X, Swain DL, Walton DB et al (2020) Simulating and evaluating atmospheric River-Induced precipitation extremes along the U.S. Pacific coast: case studies from 1980–2017. J Geophys Res Atmos 125. https://doi.org/10.1029/2019JD031554

Huntingford C, Mitchell D, Kornhuber K et al (2019) Assessing changes in risk of amplified planetary waves in a warming world. Atmospheric Sci Lett 20. https://doi.org/10.1002/asl.929

Kautz L-A, Martius O, Pfahl S et al (2022) Atmospheric blocking and weather extremes over the Euro-Atlantic sector - a review. Weather Clim Dyn 3:305–336. https://doi.org/10.5194/wcd-3-305-2022

Kornhuber K, Coumou D, Vogel E et al (2020) Amplified Rossby waves enhance risk of concurrent heatwaves in major breadbasket regions. Nat Clim Change 10:48–53. https://doi.org/10.1038/s41558-019-0637-z

Läderach A, Sodemann H (2016) A revised picture of the atmospheric moisture residence time. Geophys Res Lett 43:924–933. https://doi.org/10.1002/2015GL067449

Lehmann J, Coumou D, Frieler K (2015) Increased record-breaking precipitation events under global warming. Clim Change 132:501–515. https://doi.org/10.1007/s10584-015-1434-y

Lionello P, Scarascia L (2020) The relation of climate extremes with global warming in the mediterranean region and its North versus South contrast. Reg Envriron Chang 20:31. https://doi.org/10.1007/s10113-020-01610-z

Liu B, Tan X, Gan TY et al (2020) Global atmospheric moisture transport associated with precipitation extremes: mechanisms and

climate change impacts. Wiley Interdiscip Rev Water 7:1–25. https://doi.org/10.1002/wat2.1412
Llasat MC, Llasat-Botija M, Petrucci O et al (2013) Towards a database on societal impact of mediterranean floods within the framework of the HYMEX project. Nat Hazards Earth Syst Sci 13:1337–1350. https://doi.org/10.5194/nhess-13-1337-2013
Llasat MC, del Moral A, Cortès M, Rigo T (2021) Convective precipitation trends in the Spanish mediterranean region. Atmos Res 257 https://doi.org/10.1016/j.atmosres.2021.105581
Martínez MD, Lana X, Burgueño A, Serra C (2007) Spatial and Temporal daily rainfall regime in Catalonia (NE Spain) derived from four precipitation indices, years 1950–2000. Int J Climatol 27:123–138. https://doi.org/10.1002/joc.1369
Mastrantonas N, Herrera-Lormendez P, Magnusson L et al (2021) Extreme precipitation events in the mediterranean: spatiotemporal characteristics and connection to large-scale atmospheric flow patterns. Int J Climatol 41:2710–2728. https://doi.org/10.1002/joc.6985
Merino A, Fernández-Vaquero M, López L et al (2016) Large-scale patterns of daily precipitation extremes on the Iberian Peninsula. Int J Climatol 36:3873–3891. https://doi.org/10.1002/joc.4601
Miró JJ, Lemus-Canovas M, Serrano-Notivoli R et al (2022) A component-based approximation for trend detection of intense rainfall in the Spanish mediterranean Coast. Weather Clim Extremes 38
Muñoz C, Schultz D, Vaughan G (2020) A midlatitude climatology and interannual variability of 200- and 500-hPa Cut-Off lows. J Clim 33:2201–2222. https://doi.org/10.1175/JCLI-D-19-0497.1
Nieto R, Gimeno L, de la Torre L et al (2005) Climatological features of cutoff low systems in the Northern hemisphere. J Clim 18:3085–3103. https://doi.org/10.1175/JCLI3386.1
O'Gorman PA (2015) Precipitation extremes under climate change. Curr Clim Change Rep 1:49–59. https://doi.org/10.1007/s40641-015-0009-3
Olcina Cantos J, Díez-Herrero A (2017) Flood maps in Spain. Estudios Geograficos 78:283–315. https://doi.org/10.3989/estgeogr.201710
Papalexiou SM, Montanari A (2019) Global and regional increase of precipitation extremes under global warming. Water Resour Res 55:4901–4914. https://doi.org/10.1029/2018WR024067
Pastor F, Estrela MJ, Peñarrocha D, Millán MM (2001) Torrential rains on the Spanish mediterranean coast: modeling the effects of the sea surface temperature. J Appl Meteorol 40:1180–1195
Peña JC, Balasch JC, Pino D et al (2022) Low-frequency atmospheric variability patterns and synoptic types linked to large floods in the lower Ebro river basin. J Clim 35:2351–2371. https://doi.org/10.1175/JCLI-D-20-0394.1
Peñarrocha D, Estrela MJ, Millán M (2002) Classification of daily rainfall patterns in a mediterranean area with extreme intensity levels: the Valencia region. Int J Climatol 22:677–695. https://doi.org/10.1002/joc.747
Pérez-Zanón N, Casas-Castillo MC, Peña JC et al (2018) Analysis of synoptic patterns in relationship with severe rainfall events in the Ebre observatory (Catalonia). Acta Geophys 66:405–414. https://doi.org/10.1007/s11600-018-0126-1
Pfahl S, O'Gorman PA, Fischer EM (2017) Understanding the regional pattern of projected future changes in extreme precipitation. Nat Clim Change 7:423–427. https://doi.org/10.1038/nclimate3287
Pisso I, Sollum E, Grythe H et al (2019) The lagrangian particle dispersion model FLEXPART version 10.4. Geosci Model Dev 12:4955–4997. https://doi.org/10.5194/gmd-12-4955-2019
Queralt S, Hernández E, Barriopedro D et al (2009) North Atlantic Oscillation influence and weather types associated with winter total and extreme precipitation events in Spain. Atmos Res 94:675–683. https://doi.org/10.1016/j.atmosres.2009.09.005
Ramis C, Homar V, Amengual A et al (2013) Daily precipitation records over Mainland Spain and the Balearic Islands. Nat Hazards Earth Syst Sci 13:2483–2491
Ramos AM, Trigo RM, Tomé R, Liberato MLR (2018) Impacts of atmospheric rivers in extreme precipitation on the European Macaronesian Islands. Atmosphere 9https://doi.org/10.3390/atmos9080325
Requena AI, Jiménez-Álvarez A, García C (2023) Assessment of climate change impact on maximum precipitation in Spain. Hydrol Process 37. https://doi.org/10.1002/hyp.14803
Ribes A, Thao S, Vautard R et al (2019) Observed increase in extreme daily rainfall in the French mediterranean. Clim Dyn 52:1095–1114. https://doi.org/10.1007/s00382-018-4179-2
Richman MB (1986) Rotation of principal components. J Climatol 6:293–335. https://doi.org/10.1002/joc.3370060305
Rigo T, Llasat MC (2004) A methodology for the classification of convective structures using meteorological radar: application to heavy rainfall events on the mediterranean Coast of the Iberian Peninsula. Nat Hazards Earth Syst Sci 4:59–68. https://doi.org/10.5194/nhess-4-59-2004
Roldán-Valcarce A, Jato-Espino D, Manchado C et al (2023) Vulnerability to urban flooding assessed based on Spatial demographic, socio-economic and infrastructure inequalities. Int J Disaster Risk Reduct. https://doi.org/10.1016/j.ijdrr.2023.103894. 95:
Romero R, Ramis C, Alonso S (1997) Numerical simulation of an extreme rainfall event in catalonia: role of orography and evaporation from the sea. Q J R Meteorol Soc 123:537–559. https://doi.org/10.1256/smsqj.53901
Romero R, Ramis C, Guijarro JA (1999a) Daily rainfall patterns in the Spanish mediterranean area: an objective classification. Int J Climatol 19(199901):95–112
Romero R, Sumner G, Ramis C, Genovés A (1999b) A classification of the atmospheric circulation patterns producing significant daily rainfall in the Spanish mediterranean area. Int J Climatol 19:765–785
Senent-Aparicio J, López-Ballesteros A, Jimeno-Sáez P, Pérez-Sánchez J (2023) Recent precipitation trends in Peninsular Spain and implications for water infrastructure design. J Hydrology: Reg Stud 45. https://doi.org/10.1016/j.ejrh.2022.101308
Seneviratne SI, Zhang X, Adnan M et al (2021) Weather and climate extreme events in a changing climate supplementary material. Climate Change 2021: the physical science basis. Contribution of working group i to the sixth assessment report of the intergovernmental panel on climate change
Serrano A, García J, Mateos VL et al (1999) Monthly modes of variation of precipitation over the Iberian Peninsula. J Clim 12:2894–2919
Serrano-Notivoli R, Beguería S, Saz MÁ, de Luis M (2018) Recent trends reveal decreasing intensity of daily precipitation in Spain. Int J Climatol 38:4211–4224. https://doi.org/10.1002/joc.5562
Sousa PM, Barriopedro D, García-Herrera R et al (2021) A new combined detection algorithm for blocking and subtropical ridges. J Clim 34:7735–7758. https://doi.org/10.1175/JCLI-D-20-0658.1
Stohl A, James P (2004) A lagrangian analysis of the atmospheric branch of the global water cycle. Part I: method description, validation, and demonstration for the August 2002 flooding in central Europe. J Hydrometeorol 5:656–678
Stohl A, Forster C, Frank A et al (2005) Technical note: the lagrangian particle dispersion model FLEXPART version 6.2. Atmos Chem Phys 5:2461–2474. https://doi.org/10.5194/acp-5-2461-2005
Vázquez M, Alvarez-Socorro G, Fernández-Alvarez JC et al (2024) Global FLEXPART-ERA5 simulations using 30 million atmospheric parcels since 1980
Vicente-Serrano SM, Beguería S, López-Moreno JI et al (2009) Daily atmospheric circulation events and extreme precipitation risk in Northeast spain: role of the North Atlantic oscillation, the Western

mediterranean oscillation, and the mediterranean Oscillation. J Geophys Res Atmos 114. https://doi.org/10.1029/2008JD011492

Vicente-Serrano SM, Beguería S, López-Moreno JI et al (2010) A complete daily precipitation database for Northeast spain: reconstruction, quality control, and homogeneity. Int J Climatol 30:1146–1163. https://doi.org/10.1002/joc.1850

Vicente-Serrano SM, Azorin-Molina C, Sanchez-Lorenzo A et al (2014) Temporal evolution of surface humidity in spain: recent trends and possible physical mechanisms. Clim Dyn 42:2655–2674. https://doi.org/10.1007/s00382-013-1885-7

White D, Richman M, Yarnal B (1991) Climate regionalization and rotation of principal components. Int J Climatol 11:1–25. https://doi.org/10.1002/joc.3370110102

White S, García-Ruiz JM, Martí C et al (1997) The 1996 Biescas campsite disaster in the central Spanish pyrenees, and its Temporal and Spatial context. Hydrol Process 11:1797–1812

Yokoyama C, Tsuji H, Takayabu YN (2020) The effects of an upper-tropospheric trough on the heavy rainfall event in July 2018 over Japan. J Meteorol Soc Jpn 98:235–255. https://doi.org/10.2151/jmsj.2020-013